Calorimetric Glass Transition of Poly(2,6-dimethyl-1,5-phenylene oxide) Thin Films

Dongshan Zhou,*,†,‡ Heiko Huth,‡ Yun Gao,† Gi Xue,† and Christoph Schick*,†,‡

Nanjing National Laboratory of Microstructures, Department of Polymer Science and Engineering, School of Chemistry and Chemical Engineering, Nanjing University, Nanjing 210093, China, and Institute of Physics, Rostock University, 18051 Rostock, Germany

Received June 4, 2008; Revised Manuscript Received August 4, 2008

ABSTRACT: The glass transition of poly(2,6-dimethyl-1,5-phenylene oxide) (PPO) films with thickness ranging from about 6 nm (approximately half of radius of gyration, R_g) to 330 nm (∼29 R_g) was studied by the recently developed differential alternating current chip calorimeter with sensitivity on the order of tenths of a pJ K^{-1}. No thickness dependence of the glass temperature T_g was found for this polymer. T_gs of all the films measured in the available frequency range (∼0.5 to ∼1000 Hz) can be fit by a single Vogel−Fulcher−Tammann function in the activation plot within an uncertainty of ±3 K, thus showing no deviation from the common VFT behavior even for the thinnest film. There is also no detectable change in the shape or width of the step in heat capacity at T_g. Finally, we found that calorimetric relaxation strength at the glass transition was proportional to the thickness of the film within an uncertainty of about 25%. Consequently, we estimate the thickness of the layer deviated from the bulky behavior to be within 1.5 nm.

Introduction

There have been increasingly widespread interests in the study of the glass transition of polymer thin films, both technologically and scientifically. Technologically, polymer thin films in their glassy states have very important applications in the field of coating and protection, soft lithography, microelectronic devices, and so on. Scientifically, the theory of the nature of glass and glass transition was proposed as the deepest and the most interesting unsolved problem in solid-state theory.[1] Polymer thin films provide suitable samples to study the finite size effects on the glass transition.[2−21] People investigate the dependence of the glass transition temperature $T_g(d)$ with decreasing film thickness d until comparable with the radius of gyration (R_g) of the polymer chain, expecting to capture the characteristic correlation length of the glass transition ξ. However, prior studies on various systems have shown that with decreasing d $T_g(d)$ can increase, decrease, or remain constant depending on the details of the sample, preparation, and measurement techniques (see Richert's expansion of McKenna's arrow chart[5]). It is generally recognized that in cases of weak confinement (free surface, weak film−substrate interaction, or soft confining wall) polymer chains will show increased dynamics, e.g., shift of T_g to lower values, faster dewetting or demixing, etc. Residual stress and/or reduced level of entanglements during spin-coating of the films are also proposed as the reasons for this.[22] The dynamics of thin films has been investigated with ellipsometry,[23−27] positron annihilation lifetime spectroscopy (PALS),[8,13] Brillouin scattering,[24,28] and X-ray/neutron reflectometry.[29,30] In these studies, the temperature dependence of the independent variable is recorded at a given linear heating/cooling rate, and the change in the temperature dependence is attributed to the glass transition. Broadband dielectric spectroscopy (BDS) that gives directly the time scale of the relaxation is also recently applied to the study of ultrathin polymer films.[19,20,31−34] However, the calorimetric method, the most frequently used method in the study of bulk glasses, is seldomly used in the study of thin films, partly owning to its low sensitivity.[35]

With introduction of the silicon nitride membrane technology, performance of calorimeters has been greatly enhanced.[16,36,37] The heating rate as well as the sensitivity of the thin-film calorimeter constructed on a submicron Si_3N_x membrane microchip module can be very high mainly due to the very small addenda heat capacity of the cell itself. Allen and co-workers pioneered thin-film differential scanning calorimetry (TDSC) based on silicon nitride membranes for ultrafast heating.[16,36,37] When operated under high-vacuum conditions (ca. 10^{-5}−10^{-6} Pa), the heating rates can be as high as 10^7 K s^{-1}, and the sensitivity is several tenths of a pJ K^{-1}.[38] With this ultrafast TDSC, they studied glass transition of polystyrene, poly(2-vinylpyridine), and poly(methyl methacrylate) films with thickness ranging from hundreds of nanometers down to 3 nm. No thickness dependence of T_g was found.[15−17] Because of the nearly adiabatic conditions, controlled cooling at constant rate is not possible, as recommended to obtain glasses of well-defined history. To overcome this limitation and to perform experiments on longer time scales, Efremov performed annealing experiments to follow the relaxation processes below the glass transition after cooling.[17] These results were recently compared with variable cooling rate ellipsometric measurements.[7] It was shown that a change from VFT to Arrhenius-like behavior occurs depending on cooling rate applied in ellipsometric measurements, but no changes in the calorimetric glass transition temperature were observed. Fakhraai et al. argued that the discrepancy was due to the calorimetric measurements being performed at higher rates.[7] To obtain more direct information about the glass transition dynamics in a wider dynamic range, we have constructed a differential ac chip calorimeter with very high sensitivity (∼50 pJ K^{-1}) and wide modulation frequency range (10^{-1}−10^3 Hz).[18] The ac calorimeter is based on the same chip as was used for fast scanning calorimetry with controllable heating and cooling rates of up to 10^6 K s^{-1}.[39,40] We have previously studied the glass transition of polystyrene and poly(methyl methacrylate) films with thickness below 10 nm using the ac calorimeter.[18,41] We find that T_g is independent of the thickness, and the frequency dependence is described by the VFT behavior in the range from 1 to 10^3 Hz.

In this article, we studied the glass transition of poly(2,6-dimethyl-1,5-phenylene oxide) (PPO) thin films with thickness

* Corresponding authors. E-mail: dzhou@nju.edu.cn; christoph.schick@uni-rostock.de.
† Nanjing University.
‡ Rostock University.

10.1021/ma8012543 CCC: $40.75
Published on Web 09/27/2008

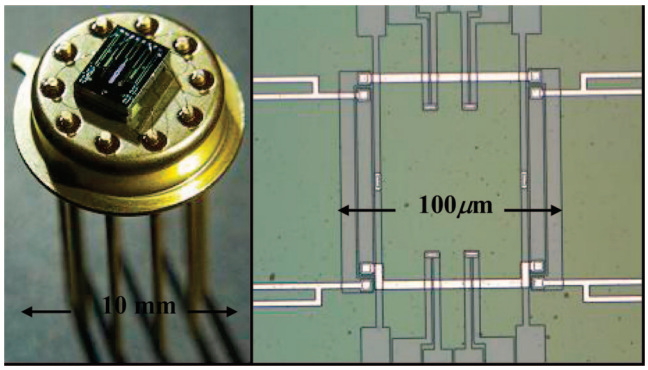

Figure 1. Left: sensor XI272 (Xensor integrations, NL[53]) in a standard TO-5 housing used in this study. Right: six thermopiles (small bright rectangles) are arranged in the central heated area (100 μm × 100 μm). The arrow points to the outer of two pairs of heater strips. The roughness in the central area is about 3.5 nm rms.

in the range from about about 330 to 6 nm. In terms of R_g, these films were 29 to 0.5 times the R_g of PPO. We find that there is no obvious shift of T_g (within 3 K) or deviation from the VFT behavior even for the thinnest film. Additionally, we find there is no detectable change in the shape or width of the transitional step of the heat capacity and that the steplike change of the apparent heat capacity at the transition is proportional to the thickness of the film within uncertainty of about 25%.

Experimental Section

1. Samples. Poly(2,6-dimethyl-1,4-phenylene oxide) (M_n = 72 000, M_w/M_n = 1.30, R_g =11.4 nm, P2501-4-DMPO) was purchased from Polymersource, Canada, and was used as received. The thin films with different thickness were prepared by spin-coating from solutions with different concentrations. The filtered (minipore, 0.2 μm) PPO/toluene solution was spin-coated onto a cleaned silica wafer for the thickness measurement and directly onto the center position of a cleaned and annealed sensor for the calorimetric measurements. The same spinning rate (3000 rpm) and spinning time (60 s) were used for all samples. The thickness of the film on the silica wafer was measured by X-ray reflectivity, and it agreed quite well with the calculated value that is based on viscosity, spinning rate, and solvent volatility.[42] Because of the similar surface properties between the sensor and the wafer, it was assumed that thicknesses were the same for the same sample preparation procedure.

The measured glass transition is strongly affected by the sample preparation details.[31−34] To avoid oxidation during annealing at higher temperatures, all measurements and annealing were performed under nitrogen flow.[31] Quasi-isothermal ac calorimetric measurements allow us to follow the multiexponential like decay of the signal amplitude during annealing of the thin films. Such decay speeds up with increasing temperature but always exists if the sample is not annealed above the bulk glass transition temperature for a long enough time. At the moment, we cannot make sure whether the decay comes from the residual solvent or the relaxation of the metastable state.[43] So unless otherwise specified, the heating/cooling traces in this work are obtained after they become stabilized. Before and after the calorimetric measurements, the sensor surface was checked by AFM, and no dewetting was observed.

2. Method. The full details of the method are described in ref 18. In this work, the sensor has a larger smoother heated area (100 μm × 100 μm), as shown in Figure 1. Another difference is that the thermopiles (six shining rectangles in right part of Figure 1) are located inside the central heated area; as a result, a correction for the temperature difference between heater and thermopile is no longer needed in this case. The frequency (ω) dependence of the radius (r_h) of the effective heated area of the sensor is recalculated[44] as $r_h = r_0 + \alpha\xi(\omega)^{-1}$, where r_0 is the static value, $\xi(\omega)^{-1}$ the characteristic length describing the decay of thermal wave in the SiN_x membrane, and α a calibration factor of about 0.2.[44] At higher frequency, $\xi(\omega)^{-1}$ becomes smaller according to $\xi(\omega)^{-1} = \sqrt{2}\xi_0^{-1}[1 + (1 + (\omega/\omega_0)^2)^{1/2}]^{-0.5}$, where ξ_0^{-1} is the value of $\xi(\omega)^{-1}$ when ω is much smaller than ω_0. ω_0 is the characteristic temperature perturbation frequency below which the thermal response of the system behaves quasi-statically. Both ξ_0^{-1} and ω_0 are solely determined by the material and fabrication parameters of the sensor.[44] Considering all the contributions discussed above, the apparent heat capacity of a single sensor plus sample in the ac calorimetry equals

$$C_{ap}(\omega) = [C_0(\omega) + C_S(\omega) + G/i\omega] \quad (1)$$

where $C_0(\omega)$ and $C_S(\omega)$ are the heat capacity of the empty sensor and sample, respectively. $G/i\omega$ is the heat loss through the surrounding gas. The heat exchange coefficient G can be obtained for any fixed temperature from the frequency dependence measured in the range, from 0.1 Hz to 1 kHz, as described in ref 45.

In the differential mode, the heat capacity of the sample is given in terms of measured quantities by

$$C_S = i\omega\tilde{C}^2(\Delta U - \Delta U_0)/SP_0 \quad (2)$$

where $\tilde{C} \equiv C_0 + G/i\omega$ is the effective heat capacity of the empty sensor, S the sensitivity of the thermopile, P_0 the heating power applied, ΔU the complex differential voltage amplitude for an empty sensor and a sensor with sample, and ΔU_0 the complex differential voltage amplitude from two empty sensors.

During the measurement, the heating power is kept constant at about 20 μW, resulting in a temperature amplitude from about 0.25 K at low frequency (<1 Hz) to 0.1 K at high frequency (>1000 Hz). $\tilde{C}$ and S change slowly in the temperature range of the glass transition. As a result, the change of sample heat capacity at glass transition can be estimated as

$$\Delta C_S = C_S(l) - C_S(g) = i\omega\tilde{C}^2[\Delta U(l) - \Delta U(g)]/SP_0 \quad (3)$$

In this study, the underlying heating/cooling rate of the thermostat is 1.0 K min^{-1}. At frequencies below 1 Hz, heating/cooling rates of 0.5 or 0.1 K min^{-1} are used to ensure that the temperature drift in the interval of data acquisition is within 0.2 K. We compared the measurements with different underlying heating/cooling rates and find that they show little effect on the measured heat capacity.

Results

Figure 2 shows a typical measurement of a 65 nm thick film. In the upper panel, where the amplitude of the differential voltage is shown, the step of the differential voltage that relates to the change of the heat capacity during the glass transition is clearly seen. In the bottom panel, the phase angle of the differential voltage is shown. As it is commonly observed in ac calorimetry, there is a peak superposed onto an underlying step.[46,47] The step is attributed to the step in heat capacity. The peak is originated from the relaxation behavior of the imaginary heat capacity during the glass transition. Both contributions can be separated as described in ref 47, and the corrected phase angle is shown in the bottom curve.

To determine the glass transition temperature T_g, we can use either the half step construction in the amplitude of the heat capacity or the peak value in the phase angle. Both give a quite similar T_g with uncertainty within ±2 K. For the PPO film with a thicness of 65 nm, the T_g measured at 20 Hz (the heater current is at 10 Hz) is 237 ± 2 °C.

In Figure 3, data for the thinnest film are shown. The peak in the phase angle for the 6 nm thick film becomes very small and comparable to the noise level of the instrument. Nonetheless, we can still see the small step in the amplitude of the voltage after smoothing with adjacent points averaging methods (Origin

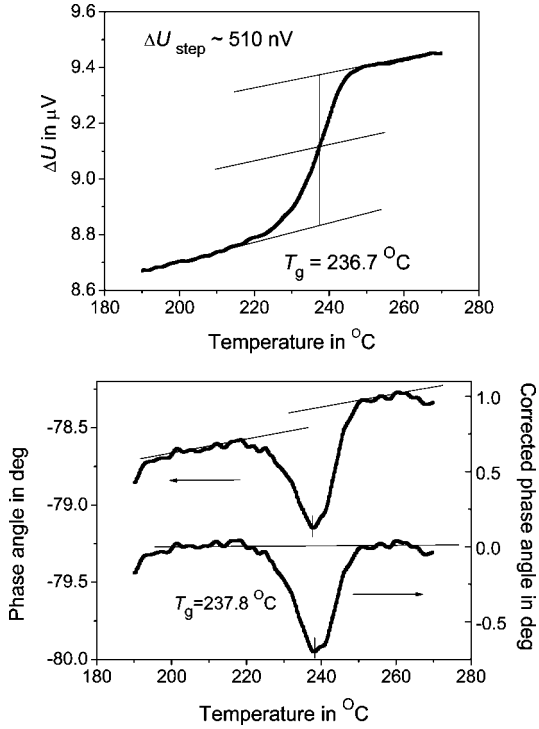

Figure 2. Amplitude (upper) and phase angle (lower) of the complex differential voltage amplitude of a thick film (65 nm). In the amplitude, a step is clearly seen. In the phase angle, a heat capacity relaxation peak is superposed onto an underlying step. The phase angle is corrected by subtraction of the contribution from the underlying step in heat capacity.[47] The T_g extracted from the half C_p construction and peak position is the same within the error limits.

8.0, 100 points). The first derivative of the smoothed curve is used to extract the T_g and the value of the amplitude step ΔU_{step}, as shown in the lower panel of Figure 3. Using different smoothing methods and parameters, we find that the variation of the T_g is about ±2 K and the variation of ΔU_{step} is about ±10%.

Figure 4 summarizes the results for all of the PPO films for all the thickness studied. The frequency dependence of T_g is shown in the activation diagram and fitted by the VFT equation We can see that for the same frequency the T_g difference

$$\log f = f_0 + \frac{B}{T_g - T_0} \tag{4}$$

between films of different thickness is only about ±3 K, a value that is similar to the uncertainty of the method. T_gs of all the films measured in the available frequency range (~0.5 to ~1000 Hz) can be fit in the activation plot by a single set of parameters for the Vogel−Fulcher−Tammann function. No obvious deviation from the VFT behavior is observed even for the thinnest film and lowest frequencies. In a recent Letter, Fakhraai, and Forrest found that the T_g's thickness dependence could be observed only at slow heating/cooling rates.[7] For polystyrene, its T_g's thickness dependence became negligible when the heating/cooling rate was above 90 K/min.[7] For our thinnest film of 6 nm, it is very difficult to perform measurement below 1 Hz, because at such low frequency the heat loss through the gas dominates the signal. To be able to compare with Fakhraai and Forrest's work, we need to decrease the frequency down to 0.01 Hz, which is possible under reduced pressure.

Discussion

The glass transition and mobility of polymers confined into very thin films has been the object of intense interest and debate

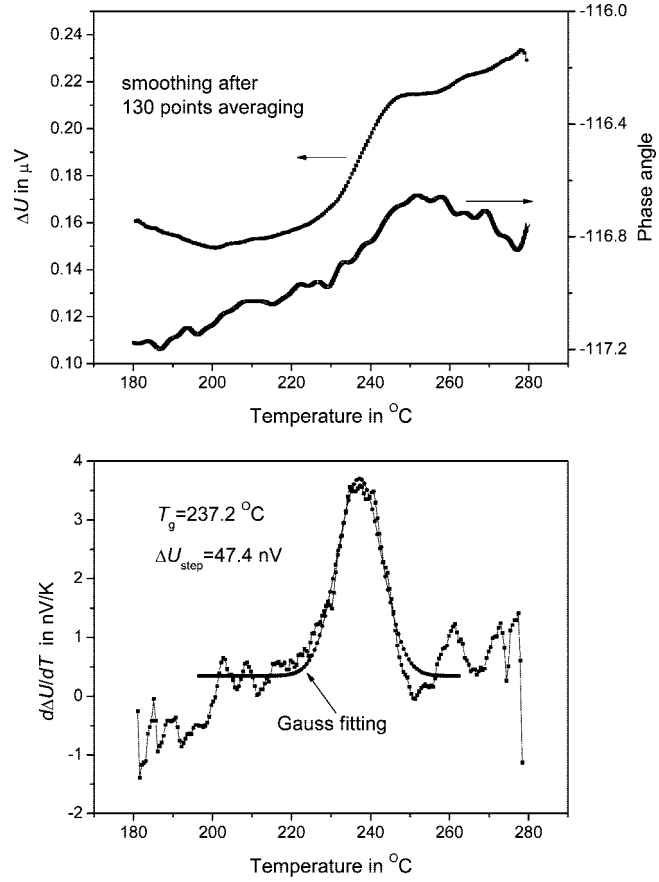

Figure 3. Upper: differential voltage amplitude measured for the thinnest film (6 nm) after 130 points averaging within each one degree and smoothing. For this thin film, the differential amplitude and its relative change at T_g decrease accordingly compared with those of the thick film. The relaxation peak appeared in the phase is too small to be visible. Lower: first derivative of the amplitude curve to extract T_g and the change of the voltage amplitude during the transition.

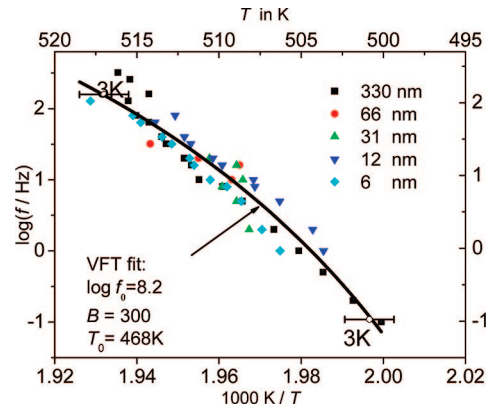

Figure 4. Frequency dependence of T_g of PPO films of different thickness. The curve represents the VFT fit with the parameters indicated in the graph.

in recent years.[2−19] There are many experimental and simulation results supporting the enhanced mobility and depression of T_g in ultrathin films[2−10] as well as many experimental results questioning this notion.[11−19] Some of the possible explanations to consolidate the discrepancy include (1) microscopic (local friction, viscoelastic properties, etc.) and macroscopic properties (heat capacity, density, etc.) investigated by different techniques do not necessarily deliver the same information regarding the glass transition;[19] (2) different techniques have different windows of length, time, or frequency scale, detecting different

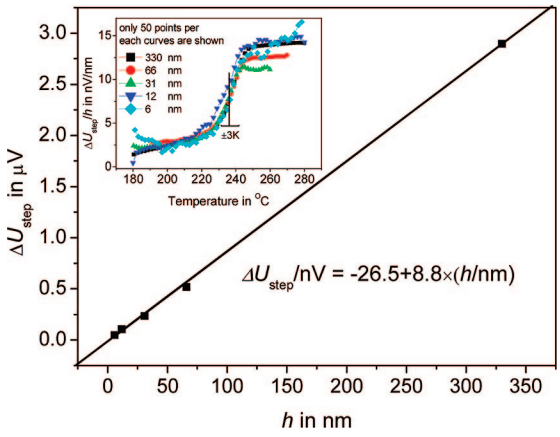

Figure 5. Step of the change of amplitude of the complex differential voltage at T_g versus film thickness from X-ray diffraction of similar samples on silicon wavers. The inset shows the measured amplitude normalized by film thickness. The curves at different film thickness collapse together with an uncertainty of about 25%.

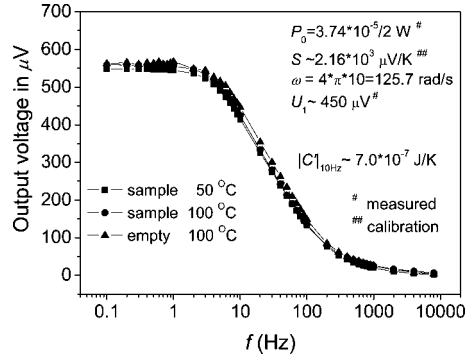

Figure 6. Frequency dependence of amplitude of complex voltage measured for one empty sensor, where effective heat capacity of the sensor can be obtained (see ref 45 and text for details). For this sensor, from the measured or calibrated values as shown in the graph, the effective heat capacity is about 700 nJ/K at the perturbation frequency of 10 Hz.

dynamics with their scale windows;[7] and (3) the different strength of the surface/interface interactions.[23] It is not the aim of this article to support or question the validity of enhanced mobility, partially because the interaction between the PPO and the substrate is not well characterized. Our goal, rather, is to measure the steplike change of heat capacity during the glass transition for films as thin as 6 nm and observe any T_g shift as a function of thickness d. From this step, we can quantify the mass, or volume, or thickness of the film under investigation.

The step height (see Figure 5) follows a linear trend with film thickness. Because the effect heated area of the sensor is little affected by the sample on it, we would expect that the measured mass is proportional to the thickness of the film. This linear trend then confirms the thickness change of the polymer film on the sensor as discussed in the Experimental Section. Also interesting is that when we normalize the curves with the respective thicknesses of the films, we find they collapse onto each other within an uncertainty of 25%, as shown in the inset to Figure 5. No detectable change in the shape or width of the step is detected.

In eq 3, we explain how to convert the measured differential voltage step into the heat capacity step. To accomplish this, we should know the value of $\tilde{C}$ and S in advance. This can be done using the frequency dependence of one single sensor, as shown in Figure 6. There are two plateaus at low and high frequencies. At low frequencies, the signal is solely determined by the heat loss through the gas. At high frequencies, the temperature amplitude decreases as $P_0/(i\omega C + G)$. As a result, there exists a certain frequency range that optimizes the sensitivity for the measurement of sample heat capacity, normally around a few tenths of a hertz. Because heat capacity of the sample (~10 nm film thickness) is much smaller than that of the addenda (~500 nm SiN_x membrane plus ~700 nm protecting SiO_2 layer), and the latter changes slowly in the temperature range of PPO's glass transition, we can safely use the effective heat capacity of the empty sensor at the sample's T_g to evaluate the step of heat capacity change during the glass transition of the sample. As shown in the legend, the heater's current frequency f is equal to 10 Hz (the power is at 20 Hz), sensitivity S is equal to 2160 μV K^{-1}, and perturbation power is 18.7 μW; then the effective heat capacity of the sensor $\tilde{C}$ equals about 700 nJ/K. With the above calibration parameters for one single sensor, we obtain the following relationship: $\Delta C_S(T_g) \sim (1.6\ \text{nJ/K})(\Delta U_{step}/\mu V)$. Since the measured step is about 47 nV, for the thinnest film of 6 nm, the change in heat capacity ΔU_{step} is about 75 pJ K^{-1}.

To compare the above measured ΔU_{step} with the value estimated based on the sample mass and its specific heat capacity, we should know the size of the effective heated area. In the case of perturbation frequency being 10 Hz (angle frequency of the thermal wave being 40π s^{-1}), $\xi(\omega)^{-1}$ equals about 200 μm with the practical material and fabrication parameters of the sensor.[44] We can then estimate the radius of the effective heated area to be about $100\sqrt{2}/2 + 0.2 \times 200 = 110.7$ μm. The effective heated volume is then about 2.3×10^{-10} cm^3, given the thickness of 6 nm. For such a volume, the change of the heat capacity should be 55 pJ K^{-1}, given the bulk density of 1 g cm^{-3} and $\Delta C_p(T_g)$ of 0.24 J g^{-1} K^{-1}.[48] The difference between the measured and estimated value is about 27%, similar to the uncertainty of the linearity approximation between ΔU_{step} and thickness h, as shown in Figure 5 and its inset. The consistency here shows that our measurements are quite reasonable. The difference may come from the underestimation of the thickness and/or the fitting parameter α. The estimation of fitting parameter can be further tested with new sensor designs, but this is beyond the scope of this article.

Another highly possible and interesting reason for the mismatch is the deviation of the surface/interface layer from the interior "bulk" behavior. Three-layer models are often applied to explain the shift of T_g from bulk value in supported thin films.[49] A liquidlike free surface and a film/substrate interface layer with different constraints are recognized as the reason for the shift of T_g. It is natural to consider their effect on the strength and shape of the glass transition, i.e., step of heat capacity. What is the "thickness" of the free surface or of the constrained interface? By PALS, De Maggio et al. find that the thickness of the free surface for the glass transition of supported polystyrene is about 2 nm[8] or, more generally, similar to the size of cooperative rearranging region.[50] Swallen et al. found a liquidlike layer in a low molecular weight compound of more than 1 nm from neutron reflectivity.[51] A similar effect was discussed for data on PS from calorimetry and dielectric spectroscopy.[20] With fluorescence probe spectroscopy, Torkelson et al. found that for PMMA both free surface and constrained interface perturbed the glassy-state structural relaxation rate at least for 100 nm and less than 250 nm into the film interior, while the thickness that the glass transition temperature was perturbed was about 25 nm.[52] These studies show that the thickness of the disturbed layer is dependent on the material itself and the property under investigation. In our case, we find that $\Delta C_S(T_g)$ was proportional to the thickness of the film within uncertainty of about 25%. Consequently, we can estimate that the deviations regarding calorimetric glass transition from the "bulk" behavior are limited to less than 1.5 nm for the thinnest film of 6 nm. Another observation from the

inset in Figure 5 is that not only does the relaxation strength scale with film thickness but the shape of the curve remains basically unchanged going from 330 to 6 nm thick film. If a gradient in mobility, probed by the calorimetric measurements, would exist, one expects to see a broadening of the glass transition interval for thinner films, but it is not observed in this study. Finally, we note that from a technical point of view determination of the thickness of the disturbed layer is still extremely challenging. With high-vacuum ellipsometry, Efremov recently showed that the measurement is highly susceptible to residual solvent or water. Even under the pressure of $10^{-6}-10^{-7}$ Torr, sorption or desorption of such impurities significantly changed the thickness of the free surface and interface.[27]

Summary

In this article, we investigated the glass transition poly(2,6-dimethyl-1,5-phenylene oxide) (PPO) films with thickness ranging from about 6 nm (approximately half radius of gyration, R_g) to 330 nm ($\sim$29 R_g) using the recently developed differential alternating current chip calorimeter. We found that T_g is independent of thickness for these films. Also, we observe no obvious deviation from the VFT behavior or change in the width of the glass transition interval. We estimated the change of heat capacity $\Delta C_S(T_g)$ based on the steplike change of the temperature amplitude during the glass transition and found that $\Delta C_S(T_g)$ was proportional to the thickness of the film within an uncertainty of about 25%. Finally, we estimate the thickness of the layer deviated from the bulky behavior to be less than 1.5 nm.

Acknowledgment. The authors gratefully acknowledge support and stimulating discussions with A. Minakov and S. Adamovsky. We also thank A. Soltow in Rostock University, Q. Tong from Kanstanz University, and Y. Ma from CNRS, Mulhouse, for the measurements of film thickness both on the silicon wafer and on the sensor. D. Zhou thanks the Alexander von Humboldt (AvH) Foundation for providing a fellowship enabling him to stay in Schick's group for 18 months. The development of the instrument was financially supported by the German Science Foundation (DFG) through several grants (Schi 331/7, 331/9, 331/14, 331/15 and 436RUS17). The work is further financially supported by the National Science Foundation of China (NSFC: 20504014, 50533020) and National Basic Research Program of China, No. 2007CB925101.

References and Notes

(1) Anderson, P. W. *Science* **1995**, *267*, 1615.
(2) Keddie, J. L.; Jones, R. A. L.; Cory, R. A. *Europhys. Lett.* **1994**, *27*, 59–64.
(3) Forrest, J. A.; Dalnoki-Veress, K. *Adv. Colloid Interface Sci.* **2001**, *94*, 167–196.
(4) Ellison, C. J.; Torkelson, J. M. *Nat. Mater.* **2003**, *2*, 695–700.
(5) McKenna, G. B. *Eur. Phys. J.—Spec. Top.* **2007**, *141*, 291–301.
(6) Fryer, D. S.; Peters, R. D.; Kim, E. J.; Tomaszewski, J. E.; de Pablo, J. J.; Nealey, P. F.; White, C. C.; Wu, W.-l. *Macromolecules* **2001**, *34*, 5627–5634.
(7) Fakhraai, Z.; Forrest, J. A. *Phys. Rev. Lett.* **2005**, *95*, 025701.
(8) De Maggio, G. B.; Frieze, W. E.; Gidley, D. W.; Zhu, M.; Hristov, A.; Yee, A. F. *Phys. Rev. Lett.* **1997**, *78*, 1524–1525.
(9) Forrest, J. A.; Dalnokiveress, K.; Stevens, J. R.; Dutcher, J. R. *Phys. Rev. Lett.* **1996**, *77*, 2002–2005.
(10) Fischer, H. *Macromolecules* **2002**, *35*, 3592–3595.
(11) Weber, R.; Zimmermann, K. M.; Tolan, M.; Stettner, J.; Press, W.; Seeck, O. H.; Erichsen, J.; Zaporojtchenko, V.; Strunskus, T.; Faupel, F. *Phys. Rev. E* **2001**, *64*, 061508.
(12) Liu, Y.; Russell, T. P.; Samant, M. G.; Stohr, J.; Brown, H. R.; Cossyfavre, A.; Diaz, J. *Macromolecules* **1997**, *30*, 7768–7771.
(13) Xie, L.; DeMaggio, G. B.; Frieze, W. E.; DeVries, J.; Gidley, D. W.; Hristov, H. A.; Yee, A. F. *Phys. Rev. Lett.* **1995**, *74*, 4947.
(14) Kim, H.; Ruehm, A.; Lurio, L. B.; Basu, J. K.; Lal, J.; Lumma, D.; Mochrie, S. G. J.; Sinha, S. K. *Phys. Rev. Lett.* **2003**, *90*, 068302.
(15) Efremov, M. Y.; Warren, J. T.; Olson, E. A.; Zhang, M.; Kwan, A. T.; Allen, L. H. *Macromolecules* **2002**, *35*, 1481–1483.
(16) Efremov, M. Y.; Olson, E. A.; Zhang, M.; Zhang, Z.; Allen, L. H. *Phys. Rev. Lett.* **2003**, *91*, 085703.
(17) Efremov, M. Y.; Olson, E. A.; Zhang, M.; Zhang, Z.; Allen, L. H. *Macromolecules* **2004**, *37*, 4607–4616.
(18) Huth, H.; Minakov, A. A.; Schick, C. *J. Polym. Sci., Part B: Polym. Phys.* **2006**, *44*, 2996–3005.
(19) Serghei, A.; Huth, H.; Schick, C.; Kremer, F. *Macromolecules* **2008**, *41*, 3636–3639.
(20) Lupascu, V.; Huth, H.; Schick, C.; Wübbenhorst, M. *Thermochim. Acta* **2005**, *432*, 222–228.
(21) Yang, H. D.; Sharp, J. S. *Macromolecules* **2008**, in press (doi: 10.1021/ma8001593).
(22) Damman, P.; Gabriele, S.; Coppee, S.; Desprez, S.; Villers, D.; Vilmin, T.; Raphael, E.; Hamieh, M.; Akhrass, S. A.; Reiter, G. *Phys. Rev. Lett.* **2007**, *99*, 036101-4.
(23) Keddie, J. L.; Jones, R. A. L.; Cory, R. A. *Faraday Discuss.* **1994**, 219–230.
(24) Forrest, J. A.; Dalnoki-Veress, K.; Dutcher, J. R. *Phys. Rev. E* **1997**, *56*, 5705–5716.
(25) Grohens, Y.; Brogly, M.; Labbe, C.; David, M. O.; Schultz, J. *Langmuir* **1998**, *14*, 2929–2932.
(26) Kim, J. H.; Jang, J.; Zin, W. C. *Langmuir* **2000**, *16*, 4064–4067.
(27) Efremov, M. Y.; Soofi, S. S.; Kiyanova, A. V.; Munoz, C. J.; Burgardt, P.; Cerrina, F.; Nealey, P. F. *Rev. Sci. Instrum.* **2008**, *79*, 043903.
(28) Forrest, J. A.; Dalnoki-Veress, K.; Dutcher, J. R.; Rowat, A. C.; Stevens, J. R. *Mater. Res. Soc. Symp. Proc.* **1996**, *407*, 131.
(29) Wallace, W. E.; Vanzanten, J. H.; Wu, W. L. *Phys. Rev. E* **1995**, *52*, R3329–R3332.
(30) Miyazaki, T.; Inoue, R.; Nishida, K.; Kanaya, T. *Eur. Phys. J.—Spec. Top.* **2007**, *141*, 203–206.
(31) Serghei, A.; Huth, H.; Schellenberger, M.; Schick, C.; Kremer, F. *Phys. Rev. E* **2005**, *71*, 061801−1-061801−4.
(32) Serghei, A.; Kremer, F. *Prog. Colloid Polym. Sci.* **2006**, *132*, 33–40.
(33) Serghei, A.; Kremer, F. *Macromol. Chem. Phys.* **2008**, *209*, 810–817.
(34) Serghei, A.; Kremer, F. *Macromol. Chem. Phys.* **2008**, *209*, 1415–1423.
(35) Blum, F. D.; Lin, W. Y.; Porter, C. E. *Colloid Polym. Sci.* **2003**, *281*, 197–202.
(36) Denlinger, D. W.; Abarra, E. N.; Allen, K.; Rooney, P. W.; Messer, M. T.; Watson, S. K.; Hellman, F. *Rev. Sci. Instrum.* **1994**, *65*, 946–958.
(37) Lai, S. L.; Ramanath, G.; Allen, L. H.; Infante, P.; Ma, Z. *Appl. Phys. Lett.* **1995**, *67*, 1229–1231.
(38) Efremov, Y.; Olson, E. A. Z. M.; Lai, S. L.; Schiettekatte, F.; Zhang, Z. S.; Allen, L. H. *Thermochim. Acta* **2004**, *412*, 13–23.
(39) Minakov, A. A.; Schick, C. *Rev. Sci. Instrum.* **2007**, *78*, 073902-10.
(40) Adamovsky, S. A.; Minakov, A. A.; Schick, C. *Thermochim. Acta* **2003**, *403*, 55–63.
(41) Huth, H.; Minakov, A. A.; Serghei, A.; Kremer, F.; Schick, C. *Eur. Phys. J.—Spec. Top.* **2007**, *141*, 153–160.
(42) Hall, D. B.; Underhill, P.; Torkelson, J. M. *Polym. Eng. Sci.* **1998**, *38*, 2039–2045.
(43) Reiter, G.; de Gennes, P. G. *Eur. Phys. J. E* **2001**, *6*, 25–28.
(44) Minakov, A. A.; van Herwaarden, A. W.; Wien, W.; Wurm, A.; Schick, C. *Thermochim. Acta* **2007**, *461*, 96–106.
(45) Minakov, A. A.; Roy, S. B.; Bugoslavsky, Y. V.; Cohen, L. F. *Rev. Sci. Instrum.* **2005**, *76*, 043906.
(46) Kraftmakher, Y. *Phys. Rep.* **2002**, *356*, 1–117.
(47) Weyer, S.; Hensel, A.; Schick, C. *Thermochim. Acta* **1997**, *305*, 267–275.
(48) Brandrup, J.; Immergut, E. H.; Grulke, E. A. *Polymer Handbook*, 4th ed.; John Wiley & Sons: New York, 1999; Vol. 2.
(49) Forrest, J. A.; Mattsson, J. *Phys. Rev. E* **2000**, *61*, R53.
(50) Donth, E. *J. Non-Cryst. Solids* **1982**, *53*, 325–330.
(51) Swallen, S. F.; Kearns, K. L.; Mapes, M. K.; Kim, Y. S.; McMahon, R. J.; Ediger, M. D.; Wu, T.; Yu, L.; Satija, S. *Science* **2007**, *315*, 353–356.
(52) Priestley, R. D.; Ellison, C. J.; Broadbelt, L. J.; Torkelson, J. M. *Science* **2005**, *309*, 456–459.
(53) van Herwaarden, A. W. *Thermochim. Acta* **2005**, *432*, 192–201.

MA8012543